www.bioforsk.no

Bioforsk FOKUS

Vol. 2
Nr. 9
2007

*Foto: Jon Schärer*

# Development of the SnowFrost model for the simulation of snow fall and soil frost

STIG MORTEN THORSEN[1]
LARS EGIL HAUGEN[2]

1 Bioforsk Vest Særheim, stig.thorsen@bioforsk.no
2 The Norwegian University of Life Sciences UMB, lars.haugen@umb.no

FOKUS

## Abstract

In the process of studying how climatic changes will influence important forage crops at high latitudes, van Oijen *et al.* (2005) developed a plant model for two grass species, timothy (*Phleum pratense L.*) and perennial ryegrass (*Lolium perenne L.*). In order to study winter survival of the plants, the plant model requires routines to simulate winter conditions, such as snow accumulation, soil frost, ice cover and soil temperature. This report describes the development of the **SnowFrost** model that simulates snow accumulation and the formation of soil frost. Routines for simulating ice encasement will be added at a later stage. The **SnowFrost** model implements a degree-day-temperature-index method in the snowmelt routines, and an energy balance approach to get an algebraic expression for soil frost formation. Our main focus when developing the winter model is to adequately simulate winter conditions from the plant's point of view, rather than accurately simulate the depths of snow cover and soil frost penetration. Simulations for a site with cold and stable winter conditions show promising results, and indicate that **SnowFrost** is suitable as a foundation for the continuing work of developing the winter routines for the plant model.



## Sammendrag

For å studere hvordan framtidige klimaendringer ved nordlige breddegrader vil påvirke viktige forgressarter, har van Oijen *m.fl.* (2005) utviklet en plantemodell for to gress arter, timotei (*Phleum pratense L.*) og flerårig raigras (*Lolium perenne L.*). For å kunne simulere plantenes evne til å overleve vinteren, må den eksisterende plantemodellen utvides med rutiner som kan simulere vinterforhold, som for eksempel dannelsen av snødekke, teledannelse, dannelse av islag oppå jorda, samt jord temperatur. Denne rapporten beskriver utviklingen av modellen **SnowFrost** som simulerer dannelsen og tiningen av et snødekke, samt dannelsen av tele i jorda. Rutiner for å simulere innkapsling av planter i is vil komme på et senere tidspunkt. **SnowFrost** modellen benytter en grad-dag-temperatur-indeks metode i simuleringen av snøsmelting, og en tilnærming via energibalanse for å få en formel for beregning av teledyp. Vi har valgt å legge vekt på å utvikle modellen med tanke på at den skal brukes i en eksisterende plantemodell. Vårt hovedfokus blir dermed å simulere vinterforholdene ut fra det som er viktig for plantene, og ikke med tanke på nøyaktige simuleringer av snødybde og teledybde. De første simuleringene som er kjørt for en forskningsstasjon med et stabilt og kaldt vinterklima viser lovende resultater. Vi vil derfor bruke **SnowFrost** som et grunnlag i den videre utviklingen av vinterrutinene til plantemodellen.

# Introduction

The global climate is changing, and during the next 100 years, the global temperature is expected to increase by 1.4 - 5.8 °C. This temperature increase is related to a parallel increase in atmospheric $CO_2$ of up to 478 - 1099 ppm (McCarthy *et al*. 2001). In Norway, the temperature rise is likely to be larger in the northern parts compared to the southern parts. Also we can expect the winter weather in Norway to be more variable, e.g. milder temperatures and more precipitation as rain (Grønås, S. 2005), which might cause more water logging, and more ice encasement and less snow cover. The effects of these climate changes on the over wintering of important agricultural crops is among the topics studied in the Norwegian Research program WINSUR (2004-2008).

As part of the WINSUR project, two of the most important grass species of silage, timothy (*Phleum pratense L.*) and perennial ryegrass (*Lolium perenne L.*), is studied. Timothy is able to survive winter conditions better than perennial ryegrass, but it shows poorer regrowth after harvesting. The reason why this is so is currently under investigation (van Oijen *et al*. 2005). This investigation involves the development of a model to adequately simulate the timothy regrowth dynamics over more than one season. In order to study the plant's abilities to withstand winter conditions like e.g. reduced photosynthesis due to snow cover, anaerobic conditions caused by ice encasement and periods of physiological drought; the current plant model will be expanded to include new routines for simulating snow cover, soil frost and ice encasement. This report describes the first version of a sub model that is going to simulate winter conditions for the plant model. The different winter conditions are organized in different modules; that is, one module simulates the snow dynamics (e.g. the formation and accumulation of snow, and snowmelt), and one module simulates soil frost.

The **SnowFrost** model currently consists of these two modules. A module that simulates the formation of an ice layer on the soil surface will be developed later.

The main objectives of the **SnowFrost** model are to produce daily values for snow $S_{depth}$, together with a lower boundary of soil frost $F_{depth}$. Important input data for the plant model is the duration of the snow cover and for how long the soil is frozen. The default parameterization of **SnowFrost** is based on previous modelling work of Riley and Bonesmo (2005) for a site located at Bioforsk Arable Crops Division, Kise, Norway (60.77 °N lat; 10.8 °E long; 127 m above sea level). The required input variables to **SnowFrost** are daily mean values for air temperature $T_{air}$ and precipitation $P$.

The plant model, including all sub models like **SnowFrost**, are implemented in the Simulink ® software package.

A table of all the symbols with their quantity and SI units used in the **SnowFrost** model is presented in appendix A.

# 1 Outline of the model, and general assumptions

**SnowFrost** consists of two main modules. One module is related to snow accumulation, packing and densification of the snow cover and snowmelt; while the other module is related to the freeze-thaw processes in the soil (see figure 1).

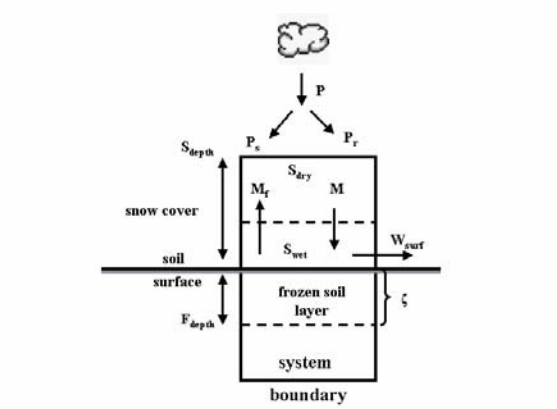


Figure 1. Description of the system simulated in the SnowFrost model.

The system's upper boundary is the soil surface during snow free periods, and the snow cover surface when snow is present. The system's lower boundary is set to the soil depth of zero annual temperature amplitude (see section 4.1). We assume that the processes simulated in the model is homogeneous throughout the site of interest. We also assume that the meteorological input (precipitation and temperature) is the same throughout the site, and that there is no spatial variation in the snow cover or in the soil composition at the site. At the moment, the soil water content $x_w$ is kept constant. In the succeeding model versions, soil water content will also be simulated. Further, the thermal conductivities of the soil $\lambda_g$ and snow cover $\lambda_s$ are kept constant. The thermal conductivity of frozen soil is assumed equal to that of unfrozen soil $\lambda_g$.

Based on the input temperature $T_{air}$ and precipitation $P$, **SnowFrost** determines the precipitation form; rain $P_r$, and snow $P_s$.

Precipitation falling as snow $P_s$ and snowmelt that refreezes within the snow cover $M_f$ constitutes the solid parts of the snow cover $S_{dry}$. The snow cover, being a porous medium, can retain a limited amount of liquid water $S_{wet}$ resulting from either rain $P_r$, or melted snow $M$ or both. If $S_{wet}$ exceeds a threshold value, referred to as the snow cover's retention capacity $f_{cap}$ (see section 2.2.3), $S_{wet}$ will add to the total snowmelt discharge $M$ in the model. In the off winter season, or when there is no snow cover present, precipitation falling as rain adds directly to the surface water $W_{surf}$.

Currently in **SnowFrost**, $W_{surf}$ does not infiltrate into the soil (soil water content being kept constant). Later this will be taken into consideration, as we will model the soil water content. At this later stage, the infiltration capacity into the soil will be influenced by the presence of soil frost.

The snow melts when there is enough energy present. **SnowFrost** use $T_{air}$ as a measure for available energy (see section 2.2.2). Based on $T_{air}$ and a degree-day factor $K_M$, **SnowFrost** calculates a daily amount of snowmelt.

Simulation of the lower boundary of soil frost $F_{depth}$ is related to the above ground temperature. If a snow cover is present, this will serve as an insulating layer, and therefore **SnowFrost** calculates an intermediate temperature $T_{surf}$ between the snow cover and the soil surface (see section 3.2).

# 2 Snow Cover

The general structure of the **SnowFrost** model is that meteorological data such as daily average temperature $T_{air}$ and daily precipitation $P$ drives the processes. The routines related to snow accumulation and snowmelt, and the numerical

values of the parameters are based on the modelling work of Riley and Bonesmo (2005).

## 2.1 Precipitation

The precipitation form is based on $T_{air}$, upper $T_{upper}$ and lower $T_{low}$ critical temperatures. Based on air temperature $T_{air}$, a fraction of water $f_w$ of the measured precipitation $P$ is calculated. If $T_{air} > T_{upper}$, all precipitation falls as rain; if $T_{air} < T_{low}$ the
precipitation fall as snow, and if $T_{air}$ is in between, the precipitation fall as a mixture of snow and water, i.e. $f_w$ is defined as

$$f_w = \begin{cases} 1.0; T_{upper} < T_{air} \\ \dfrac{T_{air} - T_{low}}{T_{upper} - T_{low}}; T_{low} \le T_{air} \le T_{upper} \\ 0; T_{air} < T_{low} \end{cases}$$

and the corresponding amounts of rain $P_r$ and snow $P_s$ are

$$P_r = f_w P$$
$$P_s = (1 - f_w) P$$

## 2.2 Snow Dynamics

### 2.2.1 Snow Accumulation

The differential equation governing the amount of dry snow and ice in the snow pack is

$$\frac{dS_{dry}}{dt} = P_s + M_f - M$$

where $S_{dry}$ is the amount of water in solid phase stored in the snow cover, $M_f$ is liquid water that freezes within the snow cover, and $M$ is the snow melt discharge.

The amount of liquid water stored in the snow pack $S_{wet}$ is governed by the equation

$$\frac{dS_{wet}}{dt} = P_r + M - M_f$$

If the entire snow pack melted instantaneously, the resulting depth of water is known as the snow water equivalent *SWE*. In **SnowFrost**, *SWE* is calculated as the sum of water stored in dry snow $S_{dry}$ and wet snow $S_{wet}$

$$SWE = S_{dry} + S_{wet}$$

The differential equation describing the change in depth of the snow cover is

$$\frac{dS_{depth}}{dt} = \frac{P_s}{\rho_{snowNew}} - \frac{M}{\rho_{snow}} - \rho_{pack} S_{depth}$$

where $S_{depth}$ is the depth of the snow cover, $\rho_{snowNew}$ is density of new snow, $\rho_{snow}$ is density of the snow pack and $\rho_{pack}$ is an empirical parameter that incorporates the increase in snow density as the snow pack ages. The density of the snow pack $\rho_{snow}$ is calculated as

$$\rho_{snow} = \frac{SWE}{S_{depth}}$$

The density of the snow pack is bounded in the model so that it doesn't exceed a maximum value of 480 kg $m^{-3}$ (note: 1 mm of precipitation equals 1 kg $m^{-2}$ ).

### 2.2.2 Melting of Snow

One area of interest where the development of snowmelt routines was necessary was in the hydrological models. Here these routines were used to estimate watershed runoff in regions with a seasonal snow cover. One of the early versions of such a snowmelt model is based on a degree-day temperature index (Melloh 1999).

In **SnowFrost** the melting of snow $M$ is based on a linear relationship between the degree-day factor $K_M$ and the air temperature $T_{air}$ above a lower base temperature for melting $T_{bm}$

$$M = \begin{cases} K_M\left(T_{air} - T_{bm}\right) \text{when } T_{air} > T_{bm} \\ S_{dry}\, perDay \ \text{ when } T_{air} > T_{bm}, \text{and} \\ \text{when } K_M\left(T_{air} - T_{bm}\right) > S_{dry}\, perDay \\ 0 \ \text{ when } T_{air} \le T_{bm} \end{cases}$$

The degree-day-temperature-index $K_M$ is the melting rate of the snow pack. This factor, together with daily air temperature $T_{air}$, substitutes the energy balance of the snow pack, i.e. air temperature is used as an indicator of the surface energy balance. The factor $K_M$ is calculated as

$$K_M = K_{\min}\left(1 + K_{cum}\rho_{snow}\right) \ \text{ when } \ K_M \le K_{\max}$$

where $K_{max}$ and $K_{min}$ are maximum and minimum values for $K_M$, respectively, and $K_{cum}$ is an empirical parameter (Riley & Bonesmo 2005).

#### 2.2.3 Liquid Water Retention Capacity of the Snow pack

The snow pack is able to retain a certain amount of liquid water. The maximum value $f_{capMax}$ of this retention capacity $f_{cap}$ (dimensionless) is when the snow pack consists of only fresh snow. The retention capacity decrease as the snow pack changes character due to a combination of compression, aging and the addition of liquid water either from precipitation as rain or melted snow. In the **SnowFrost** model, these changes are assumed captured by the change in the density $\rho_{snow}$ of the snow pack (Riley & Bonesmo 2005). Liquid water is retained within the snow pack until the maximum limit is reached. Liquid water exceeding this limit percolates through the snow pack and adds to the amount of liquid water on the soil surface. The retention capacity $f_{cap}$ is a function of snow density $\rho_{snow}$, the empirical parameter $C_{cum}$, and the parameters $f_{capMax}$ and $f_{capMin}$

$$f_{cap} = f_{capMax}\left(1 - C_{cum}\rho_{snow}\right) \text{ when } f_{cap} > f_{capMin}$$

#### 2.2.4 Refreezing of Melted Snow

Along the lines of the snowmelt routine, all liquid water present within the snow pack may freeze as long as the air temperature drops below a lower base temperature for freezing $T_{bf}$. The rate of water that refreezes $M_f$ is calculated as

$$M_f = \begin{cases} K_f\left(T_{bf} - T_{air}\right) & \text{when} \quad T_{air} < T_{bf} \\ 0 & \text{when} \quad T_{air} \ge T_{bf} \end{cases}$$

where $K_f$ is the refreezing parameter.

#### 2.2.5 Surface Runoff

Liquid water on the soil surface comes from either rain or melted snow. At the moment, infiltration into the soil is not implemented so all excess water runs out of the simulated system as surface runoff. The rate of surface runoff $W_{out}$ is calculated as

$$W_{out} = S_{wet}\, perDay \ + M + P_r - M_f - f_{cap}S_{dry}$$

where $S_{wet}$ is the amount of liquid water present in the snow pack, $P_r$ is rain, $M$ is the rate of snowmelt, $S_{dry}$ is the amount of solid water (snow and ice) in the snow pack this day, and $f_{cap}$ (fraction) is the amount of liquid water the snow pack can retain.

## 3 Frost Formation in the Soil

In a closed system, the phase of any substance (gaseous, liquid and solid) is governed by the pressure and temperature within this system, e.g. the phase of water in a closed cylinder. Although the soil can not be regarded as a closed system,

soil water can occur in all phases throughout the course of one year. When considering soil water, both the temperature and pressure (the pressure of soil water is often referred to as the soil water potential) varies over the season. A drop in soil temperature below 0 °C, may cause soil water to freeze. This temperature is referred to as $T^*$, the freezing temperature. However, both the amount of dissolved salts in the soil water and the soil water potential has an influence on the freezing point of soil water. This change in the freezing point is known as freeze-point depression.

Soil frost in **SnowFrost** is regarded as one homogeneous layer of frozen soil that originates at the soil surface and expands downwards to the lower frost boundary $F_{depth}$. The thickness of the frozen soil layer is called $\zeta$ (see figure 1). We use equation (22) in the derivation of an algebraical expression for the depth of the frozen soil layer. **SnowFrost** simulates the lower frost boundary under the following assumptions:

- a one-dimensional stationary flow of energy from the lower frost boundary towards the soil surface
- a constant heat flow at the system's lower boundary due to geothermal conditions $Q_g$
- ignore variation in soil thermal conductivity $\lambda_g$
- no freeze-point depression, i.e. $T^*$ is equal to 0 °C regardless of the salt concentration and the soil water potential
- a constant soil water content at field capacity throughout the winter

In the process of calculating $F_{depth}$, under the conditions of soil frost formation, we assume a linear variation in soil temperature $T(z,t)$ with respect to depth below the soil surface $z$ (note: during periods of no snow cover $T_{surf} = T_{air}$)

**Equation 1**

$$T(z,t) = T_{surf} + \frac{T^* - T_{surf}}{\zeta} z$$

where $T_{surf}$ is the temperature just above the soil surface at time $t$, and $\zeta$ is the depth of the frost layer from the soil surface to $T^*$ (the lower frost boundary). Equation (1) is valid only when soil frost is present (i.e. when $\zeta > 0$).

The melting of ice requires energy (335 kJ pr kg ice) and thus when water freezes; the same amount of energy is released. This energy is called latent heat of fusion $L_f$. If we consider a unit volume $V$ of soil where $m_w$ is the mass of water in this soil volume, we can express the rate at which $L_f$ is released as

**Equation 2**

$$L_f \frac{\partial m_w}{\partial t}$$

where $\frac{\partial m_w}{\partial t}$ represents the change in soil water mass $m_w$ with respect to time as soil water freeze. The freezing of water in a volume of soil entails a change in the amount of liquid water present. If we regard the area $A$ of a soil column and d$\zeta$ as a small increase in the frost layer, we can express the subsequent increase in ice content in this small volume d$V$ as

**Equation 3**

$$\mathrm{d}V = A\mathrm{d}\zeta$$

We denote the volume fraction of liquid soil water present in $V$ by $x_w$, and $\rho_w$ is the density of water. Thus we can express $\partial m_w$ from equation 2 as

**Equation 4**

$$\partial m_w = x_w \rho_w A \partial \zeta$$

Dividing the above equation by the unit area $A$, and inserting equation 4 into equation (2) we

obtain the following expression for the heat flux density

**Equation 5**

$$Q_E = x_w \rho_w L_f \frac{\partial \zeta}{\partial t}$$

where $Q_E$ is the latent heat flux density released when the soil water $x_w$ in the volume d$V$ freeze (see figure 3).

In the model, the freezing of soil water is initiated when the air temperature just above the soil surface $T_{air}$ drops below 0 ˚C (see figure 2). When the soil cools down, the heat flux density $Q_{cool}$ is directed upwards from the soil towards the air just above the soil surface. Now, we can envisage the soil surface as the active surface through which the energy flows. As heat keeps flowing through this active surface, the soil cools down. The soil temperature $T(z,t)$ decreases, and when $T(z,t)$ reaches $T^*$, water in the soil surface layer freezes.

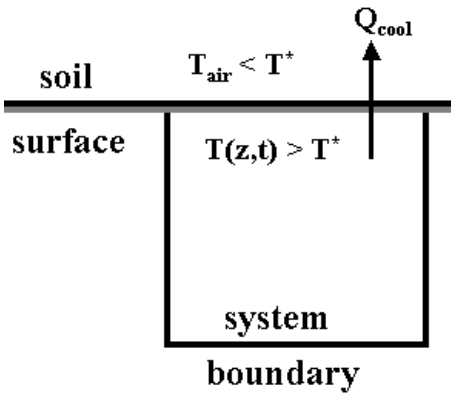


Figure 2. The figure illustrate the initiation of soil frost with $T_{air}$ < T*.

Some of the heat that is extracted at the soil surface will be counterbalanced and retained within the soil due to $L_f$ (heat released when soil water freezes). This somewhat inhibits the freezing process, and results in the latent heat flux density $Q_E$ from equation (5). If more energy is extracted at the soil surface than $L_f$ can counterpart, i.e. $Q_{cool} > Q_E$, the active surface (where the heat from freezing counterbalances the upward heat flux due to the temperature difference between soil and air) will shift downwards until it's counterbalanced again, and a new equilibrium between the heat extracted $Q_{cool}$ and $Q_E$ is established; resulting in the formation of a frozen soil layer of depth d$\zeta$ (see figure 3).

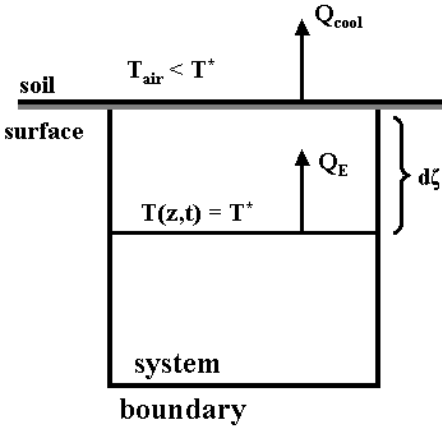


Figure 3. A frozen soil layer of depth d$\zeta$ is developing. $Q_E$ is released when the soil water in this layer freeze.

If the cold conditions with $T_{air} < T^*$ prevails, the thickness of the frozen soil layer d$\zeta$ will increase (see figure 4).

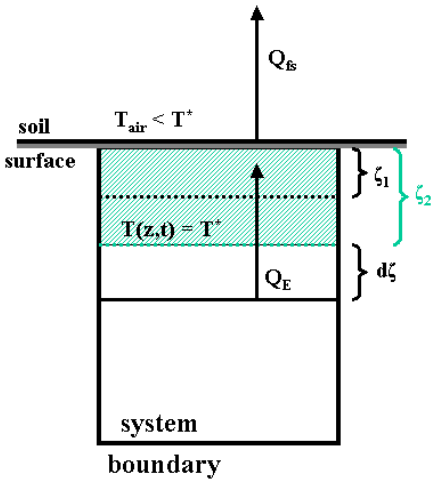


Figure 4. Development of a frozen soil layer: $\zeta_1$ and $\zeta_2$ are the thickness of the frozen soil layer at two different times $t_1$ and $t_2$, respectively. $Q_E$ is the latent heat flux density from the small volume d$V$ of depth d$\zeta$, and $Q_{fs}$ is the heat conducted through the frozen soil layer (shaded area).

From the one-dimensional heat equation, equation (15) in Appendix B.1 we have the heat flux density

$$Q = -\lambda \frac{\partial T}{\partial z}$$

We obtain $\frac{\partial T}{\partial z}$ in this equation by differentiating equation (1) with respect to z, that is

$$\frac{\partial T}{\partial z} = \frac{T^* - T_{surf}}{\zeta}$$

Now we can express the heat flux density $Q_{fs}$ through the frozen soil layer $\zeta$ (the shaded area in figure 4) by inserting the above expression in equation (15) to obtain

**Equation 6**

$$Q_{fs} = -\lambda_g \frac{\partial T}{\partial z} = -\lambda_g \frac{T^* - T_{surf}}{\zeta}$$

Due to the cooling of the soil, heat released by the freezing process $Q_E$ is conducted through the frozen layer. In figure 4, $Q_{fs}$ is the heat flux density through this frozen layer of depth $\zeta_2$. This heat flux density at soil depth $z = \zeta_2$ is balanced by the latent heat flux density $Q_E$, and by equating equations (6) and (5) we obtain

**Equation 7**

$$Q_E = Q_{fs}$$

$$-x_w \rho_w L_f \frac{\partial \zeta}{\partial t} = -\lambda_g \frac{T^* - T_{surf}}{\zeta}$$

(note: $Q_{fs} = 0$ when $\zeta = 0$).

Now, suppose the lower frost boundary is zero when we start the simulation at time $t_0$, and at time $t$, it has reached the depth $F_{depth}$, and we have a frozen soil layer of thickness $\zeta$. An estimate of the depth of this frost layer can be found by rearranging equation (7), and performing the integrations as follows

**Equation 8**

$$\int_0^{F_{depth}} \zeta \, d\zeta = \frac{\lambda_g}{x_w \rho_w L_f} \int_{t_0}^{t} \left(T^* - T_{surf}\right) dt$$

We can simplify the integral on the right hand side in the above equation above by assuming that soil water freeze at 0 °C, which means setting $T^* = 0$. By expanding the differential d$t$ to the difference $\Delta t$ we find an approximation of the integral on the right hand side in equation (8). The increment $\Delta t$ indicates a time interval of 1 day. When calculating the soil frost, only frost days ($T_{surf} \leq 0$ °C) are considered (note: during periods of no snow cover $T_{surf} = T_{air}$, and when a snow cover is present $T_{air}$ represents the air temperature just above the snow surface). We call the integral on the right hand side in equation (8) $F(t)$, i.e.

$$F(t) = \int_{t_0}^{t} \left(T^* - T_{surf}\right) dt$$

which under the assumptions from above simplifies to

$$F(t) \approx \sum_i \left(-T_{surf} \Delta t\right)_i$$

where the index $i$ indicates days with frost formation (Johansen 1976). Solving the integral on the left hand side in equation (8) produces an algebraic expression for estimating the depth of the lower frost boundary

**Equation 9**

$$F_{depth} = \sqrt{\frac{2\lambda_g F(t)}{x_w \rho_w L_f}}$$

Here the simulated frost depth $F_{depth}$ is a function based on daily average values for air temperature above the soil surface on frost days.

## 3.1 Ground Heat Flux

The temperatures in the uppermost soil layers follow with some time lag, the diurnal variation in the air temperature. This temperature variation makes out a wavelike pattern, and also the amplitude of this temperature wave tends to decrease with soil depth. The annual soil temperatures also follow a wavelike pattern, in correspondence with the annual solar cycle. Figure (5) shows the annual temperature-wave for the Kise site, where the mean annual temperature for the period 1.1.91 - 31.12.02 was 4.8 °C. The

soil depth at which there is practically no change in the amplitude of this temperature-wave is termed depth of zero annual amplitude. According to Jansson and Karlberg (2001), we assume that the system's lower boundary condition for heat conduction can be given as a constant heat flux density equal to a geothermal contribution parameter $Q_g$.

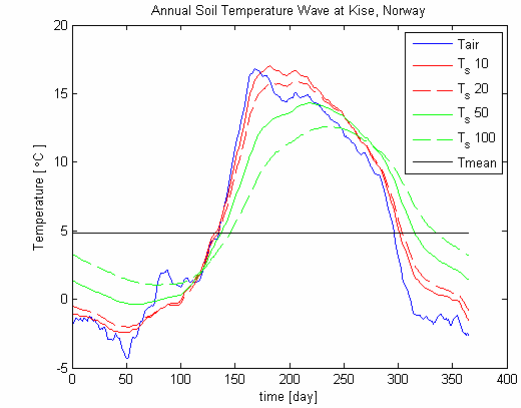


Figure 5. Annual temperature wave at Kise, Norway (1.1.92 - 31.12.92). $T_{air}$ is daily mean air temperature, $T_{mean}$ = 4.8 °C is mean air temperature over the normal period 1961 - 1990, $T_s10$, $T_s20$, $T_s50$ and $T_s100$ are mean daily soil temperatures at depths of 10 cm, 20 cm, 50 cm, and 100 cm, respectively.

This heat $Q_g$ will add to $Q_E$ and to a certain degree inhibit and slow down the formation of soil frost (see figure 6)

{energy in at soil surface} =

{energy in at lower surface}

$Q_{fs} = Q_E + Q_g$

When including the ground heat flux density $Q_g$, the energy balance from equation (7) can be expressed as

**Equation 10**

$$Q_{fs} = Q_g + Q_E$$

$$-\lambda_g \frac{T^* - T_{surf}}{\zeta} = -\left(Q_g + x_w \rho_w L_f \frac{\partial \zeta}{\partial t}\right)$$

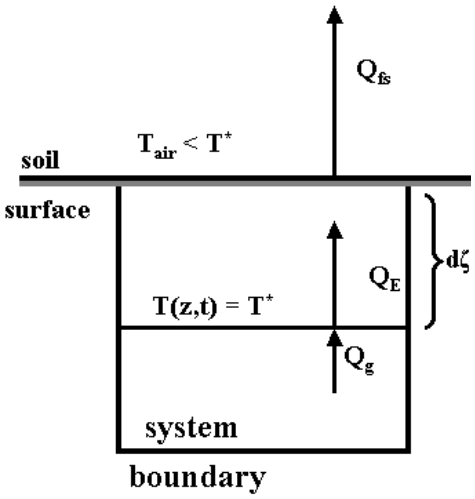


Figure 6. The formation of soil frost is inhibited due to a geothermal heat contribution $Q_g$.

Rearranging equation (10), and performing the same integration as above in equation (8) we obtain

**Equation 11**

$$\int_0^{F_{depth}} \zeta \mathrm{d}\zeta = -\frac{Q_g}{x_w \rho_w L_f} \int_{t_0}^{t} \zeta \mathrm{d}t + \frac{\lambda_g}{x_w \rho_w L_f} \int_{t_0}^{t} \left(T^* - T_{surf}\right) \mathrm{d}t$$

By solving equation (11) we obtain

**Equation 12**

$$\left(F_{depth}\right)^2 + \frac{2Q_g\left(t - t_0\right)}{x_w \rho_w L_f} F_{depth} - \frac{2\lambda_g F(t)}{x_w \rho_w L_f} = 0$$

The simulated frost depth $F_{depth}$ in **SnowFrost** is based on equation (12).

Based on measurements at a site in Aas, Norway, (59.66 °N lat; 10.78 °E long; 70 m above sea level), using constant soil water content $x_w$ = 0.4, Olsen and Haugen (1997) estimated the soil thermal conductivity $\lambda_g$ to 2 W m$^{-1}$ K$^{-1}$, and by assuming stationary conditions, they estimated the constant ground heat flux $Q_g$ to 0.3 MJ m$^{-2}$ day$^{-1}$ for this site. Stationary conditions means that when the thickness of the frozen soil layer cease to increase, that is when $Q_E$ = 0 because no additional

ice is formed, there exists an equilibrium between the heat extracted at the soil surface $Q_{fs}$ and heat added from the ground beneath $Q_g$, i.e.

{energy out at soil surface} =

{energy in at lower frost boundary}

$$Q_{fs} = Q_g$$

Since $Q_g$ persists, this means that ground heat $Q_g$ that enters the frozen soil layer at the lower boundary is transported through this layer without any further increase in the layer's temperature (i.e. stationary conditions), see figure (7).

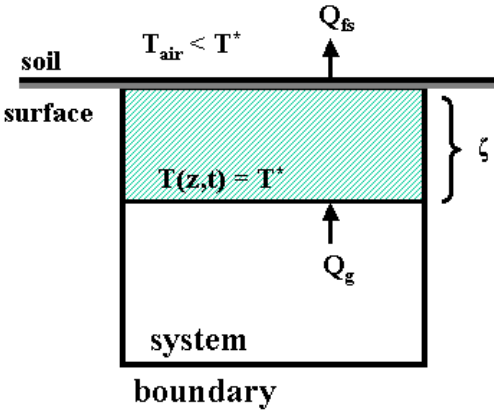


Figure 7. Stationary conditions where heat flux density entering at the lower frost boundary $Q_g$ is the same as the heat flux density extracted at the soil surface $Q_{fs}$.

## 3.2 Effect of Snow Cover on Soil Frost Formation

The presence of a snow cover has influence on the formation of soil frost, due to its insulating effect. According to Jansson and Karlberg (2001), we assume a steady state heat flow through the frozen soil layer and the snow pack, see figure 8. This means that the heat flux density through the frozen soil $Q_{fs}$ equals the heat flux density through the snow pack $Q_{snow}$, and thus from equations (15) and (6)

$$Q_{fs} = Q_{snow}$$

$$-\lambda_g \frac{T^* - T_{surf}}{F_{depth}} = -\lambda_s \frac{T_{surf} - T_{air}}{S_{depth}}$$

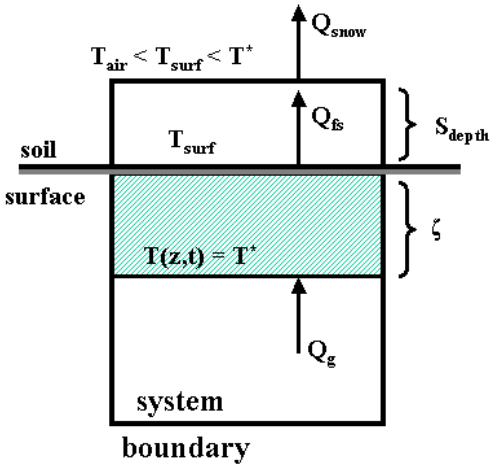


Figure 8. The steady state heat flow through the frozen soil layer and the snow cover, where $Q_g = Q_{fs} = Q_{snow}$.

where the thermal conductivities of the frozen soil layer and the snow cover (new snow) are $\lambda_g$ and $\lambda_s$, respectively, and $F_{depth}$ and $S_{depth}$ is the depths of the frozen soil layer and the snow cover both at time $t$, respectively. According to our assumption $T^* = 0$ °C, we can rearrange the above equation and obtain

**Equation 13**

$$T_{surf} \approx \frac{T_{air}}{1 + \frac{\lambda_g S_{depth}}{\lambda_s F_{depth}}}$$

The thermal conductivity of snow is closely related to the snow density. For simplicity, in **SnowFrost** we use $\lambda_S$ for new snow. This is considerably lower than $\lambda_g$ for the sand-type soil with a soil water content $x_w$ of 0.4, which we use in **SnowFrost**. According to Jansson and Karlberg (2001) a reasonable estimate for the ratio $\lambda_g$ / $\lambda_s$ in our situation seems to be $\lambda_g$ / $\lambda_s \approx 10$ , where in **SnowFrost** $\lambda_s$ is fixed at a constant value. As the snow density changes due to climatic factors, so will $\lambda_s$. Further testing of **SnowFrost** will indicate if we should make $\lambda_s$ a function of liquid water content in the snow cover $S_{wet}$, and snow density $\rho_{snow}$ , or if the current simplification suffices.

We have from equation (8) that the depth of the frozen soil layer is related to the history of the air temperature above the soil surface $T_{surf}$. The surface temperature from equation (13) is in turn related to whether or not soil frost is present. In the case of a present snow cover, but no soil frost, the temperature in the void between the soil surface and the bottom of the snow cover will lie around 0˚C. To incorporate this we have introduced an additional empirical expression for $T_{surf}$ to preserve the insulating effect of the snow cover. The $\gamma$ parameter ensures that $T_{surf}$ stays close to 0˚C (note: in **SnowFrost** when soil frost is present $F_{depth} < 0$)

$$T_{surf} = \begin{cases} T_{air} e^{-\gamma S_{depth}} & \text{if } F_{depth} = 0 \\ \dfrac{T_{air}}{1 - 10 \dfrac{S_{depth}}{F_{depth}}} & \text{if } F_{depth} < 0 \end{cases}$$

Soil frost increases as long as $T_{surf}$ or $T_{air}$ is below 0˚C. Soil frost decreases either as a function of the surface temperature (when this is above 0˚C), or due to a constant contribution of heat from the ground $Q_g$ (the latter is small compared to the first), or as a function of both. Heat contribution from infiltrating rainwater is currently not considered in the model.

### 3.3 Thaw Process

The thaw of soil frost is a complex process. A frozen volume of soil thaws when it absorbs more energy than what is extracted from it during the freezing process. Among the sources of available energy to heat frozen soil is absorbed radiation, the exchange of sensible heat from warmer ambient air, geothermal heat from unfrozen lower soil layers, and percolating rainwater with a higher temperature. The thaw routine in **SnowFrost** is currently very simple. A certain amount of energy melts a certain amount of ice.

We thus simulate soil thaw $S_{thaw}$ along the same lines as for soil frost; saying that days when $T_{air} > 0$˚C yields a certain amount of soil thaw. We calculate

**Equation 14**

$$S_{thaw} = \sqrt{\frac{2\lambda_g Thaw(t)}{x_w \rho_w L_f}}$$

where $Thaw(t) \approx \sum_i \left(-T_{air}\Delta t\right)_i$ (the index $i$ indicates days with soil thaw), and $S_{thaw}$ is an algebraic expression estimating the amount of soil thaw. By subtracting $S_{thaw}$ from *Fdepth* we simulate the process of soil thaw.

# 4 Simulation Results and Discussion

The **SnowFrost** model is based on the previous modelling work of Bonesmo and Riley (2005) for Kise. We used Kise as a test site to see how the model behaves with relatively stable winter conditions. The parameter values used for the preliminary runs of **SnowFrost** are adapted from Bonesmo and Riley. In the snowmelt routine we use a base temperature for snowmelt $T_{bm}$. According to Melloh (1999), the degree-day-temperature-index approach for snowmelt adopted in **SnowFrost** serves best in forested rather than open areas.

Observations on the lower frost boundary were obtained using a Gandahl gauge. During snowmelt in spring, the snow adjacent to the Gandahl gauge apparatus might melt faster, creating a funnel and thus causing the soil frost to thaw more rapidly around the gauge apparatus compared to the rest of the field (Colleuille and Gillebo, 2002). On cold nights in early spring we can observe the opposite situation around the funnel, namely additional soil frost formation. These situations increase the uncertainty in the soil frost observations during snow melt periods.

Regarding the thawing routine, although this approach is quite crude, the simulations of the freezing and thawing processes are satisfactory at the moment. They will be revised in a later version of the model.

Figures 9a-9f show the results from three runs of **SnowFrost** at Kise. The simulation periods are 1 June (day number 1 in figures 9a-9f) to 31 May (day number 365 in figures 9a-9f) the following year (note: in figure 9c the plot period is 01.10.1995 - 31.05.1996). Each figure consists of two panels; in the upper panel the blue solid line shows the air temperature $T_{air}$ *after* being smoothed by a moving average; the bar diagram shows precipitation *P*.

The lower panel shows simulated snow cover $S_{depth}$ (solid blue line), observed snow cover (dotted blue line), simulated frost depth $F_{depth}$ (solid black line), observed frost depth (dotted magenta line). To get an impression
of when the soil becomes frost free, we have plotted the times when the observed soil temperature at four different depths (10 cm, 20 cm, 50 cm and 100 cm) changes from negative to positive. The symbols (in magenta colour) corresponding to these times are:
o for 10 cm, * for 20 cm, ◊ for 50 cm, and
□ for 100 cm. Enclosed in red boxes in the lower panels is the total frost sum during the simulation period. This frost sum was calculated as

$$\sum T_{air} \Delta t$$

on days where $T_{air} < 0^{\circ}C$. To get a preliminary evaluation of how **SnowFrost** performs, for each run we calculated the root mean square error (*RMSE*) and the squared Pearson correlation *r* for snow cover $\left( RMSE_{snow} \text{ and } r^2_{snow} \right)$ and soil frost $\left( RMSE_{frost} \text{ and } r^2_{frost} \right)$, respectively. The *RMSE* was calculated as

$$RMSE = \frac{1}{\overline{O}} \sqrt{\frac{\sum_{i=1}^{n} \left(O_i - Sim_i\right)^2}{n}}$$

where $\overline{O}$ is the mean of the observations, $O_i$ are the *n* observations, and $Sim_i$ are the corresponding simulation values. A perfect match between observations and simulated values would yield *RMSE* = 0. See table 1 for the results of each run.

**Table 1: Simulation results**

| Simulation period | Snow | | Frost | |
|---|---|---|---|---|
| | *RMSE* | $r^2$ | *RMSE* | $r^2$ |
| 01.06.93 - 31.05.94 | 0.46 | 0.89 | 0.52 | 0.09 |
| 01.06.94 - 31.05.95 | 1.31 | 0.58 | 0.35 | 0.08 |
| 01.06.95 - 31.05.96 | 0.77 | 0.91 | 0.12 | 0.91 |
| 01.06.96 - 31.05.97 | 1.30 | 0.63 | 0.30 | 0.69 |
| 01.06.97 - 31.05.98 | 1.45 | 0.76 | 0.25 | 0.02 |
| 01.06.98 - 31.05.99 | 1.01 | 0.79 | 0.27 | 0.81 |

Table 1. Column 1 show the simulation period for each run (note: run # 3). Column 2 shows root mean square error for snow $RMSE_{snow}$. Column 3 show squared Pearson *r* for snow. Column 4 shows root mean square error for frost $RMSE_{frost}$. Column 5 show squared Pearson *r* for frost.

In figure 9a and 9b we can see the simulated snow cover captures the variation in observed snow cover quite well both these winters, although it is overestimated in 1993-1994 and underestimated in 1994-1995. In 1993-1994 and 1994-1995 the simulated frost layer appears earlier than observed. The maximum value of $F_{depth}$ does not differ too much from the observed maximum frost depth for 1993-1994, but is underestimated for 1994-1995. The timing of complete snowmelt is somewhat earlier than observed in the winter of 1993-1994, and quite good for 1994-1995. The timing of soil thaw is way too early in 1993-1994, but quite good in 1994-1995.

In figure 9c the simulated snow dynamics for 1995-1996 is quite good. For both figures 9c and 9d, the expanding period of soil frost is also captured nicely, although the timing of soil thaw comes at the end of both simulation periods. In figure 9d, the simulated snow dynamics are captured to some extent. The timing of simulated soil thaw is quite good this period.

In figure 9e, the snow dynamics is simulated nicely. There are several freeze/thaw incidents this period, but $F_{depth}$ still resembles the tendency in the observed soil frost. The simulated soil thaw comes too late this period. In figure 9f, the snow dynamics is captured nicely, although underestimated due to complete melt approximately in mid winter. The $F_{depth}$ is underestimated this period. Simulated soil thaw also comes too late in this period.

The variations in the snow cover and soil frost simulations are enhanced by inaccuracy in snow depth and frost depth measurements as well as in the model itself. The snow cover and its properties are of great importance when estimating for instance the depth of the soil frost, and soil temperature during winter (Kennedy and Sharrat, 1998). Throughout each simulation we assume the thermal conductivity of the snow cover $\lambda_s$ to be fixed. We use a value for $\lambda_s$ that corresponds to that of new snow. Obviously, $\lambda_s$ changes as the physical properties of the snow cover change. One consequence of this is that the insulation effect of the snow cover is too big. This then leads to an underestimation of the frost depth. Another aspect regarding the simulation of snow cover is in relation to actual snow density and actual snow depth. These variables are difficult to measure in practice. The depth of the snow cover affects the insulation ability, and one of the factors affecting the thermal conductivity is the density of the snow cover. Both the depth and the thermal conductivity of the snow cover affect the soil frost dynamics. In the continuing work we aim to improve the model's ability to estimate duration of the snow cover, i.e. the timing of snowmelt, and the timing of soil thaw.

Among the issues we will address in the succeeding modelling work are: add a tipping-bucket routine for the simulation of soil water processes; implement the effects of soil frost on the soil infiltration capacity, add a module for the simulation of ice encasement of plants, replace the fixed $\lambda_g$, $\lambda_s$ and $\rho_{snow}$ with functions relating them to the liquid water content of soil and snow, include new routines for the simulation of the soil

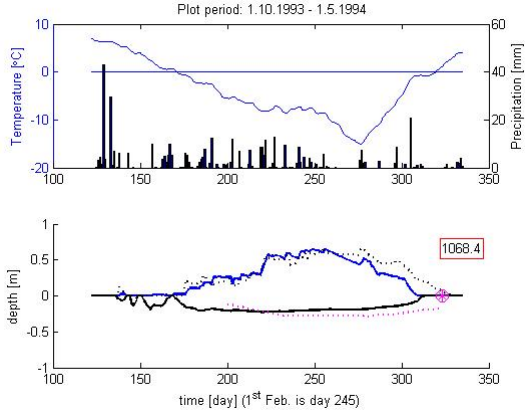


Figure 9a. Simulation results for the winter of 1993-1994. In the upper panel: solid line is smoothed $T_{air}$, bars represent precipitation. Lower panel: solid lines represent $S_{depth}$ and $F_{depth}$; dotted lines represent observed snow cover depth and depth of soil frost, respectively. Magenta symbols represent times when the observed soil temperature at four depths (o = 10 cm, * = 20 cm, ◊ = 50 cm, ▫ = 100) changes from negative to positive. Number in the red box represents frost sum.

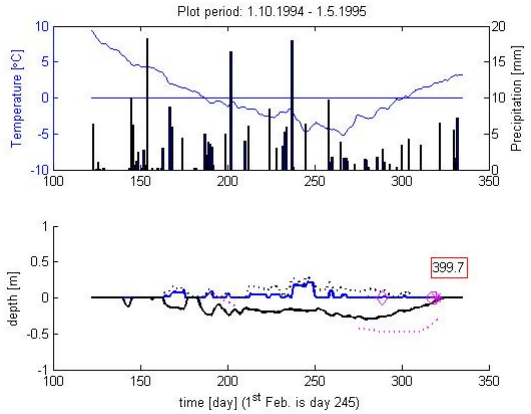


Figure 9b. Simulation results for the winter of 1994-1995.

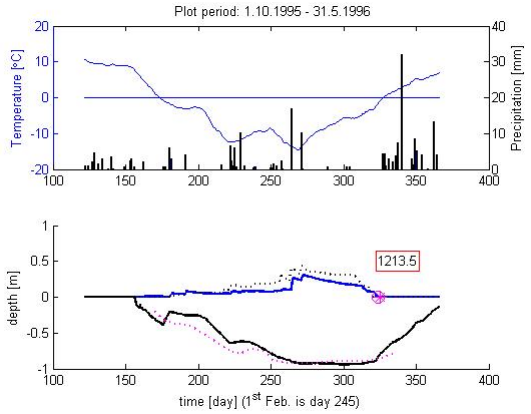


Figure 9c. Simulation results for the winter of 1995-1996. Note that plot period was 1.10.95-31.05.96.

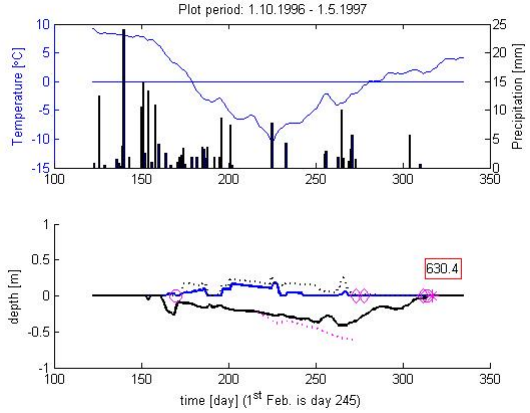


Figure 9d. Simulation results for the winter of 1996-1997.

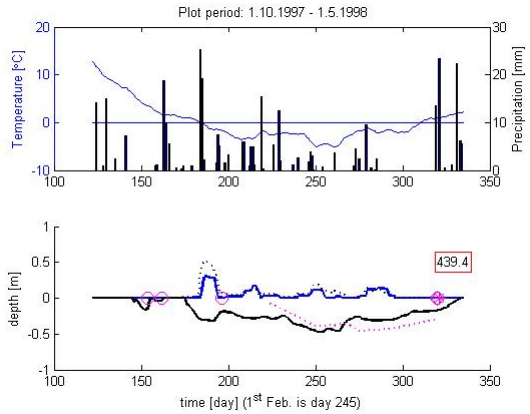


Figure 9e. Simulation results for the winter of 1997-1998.

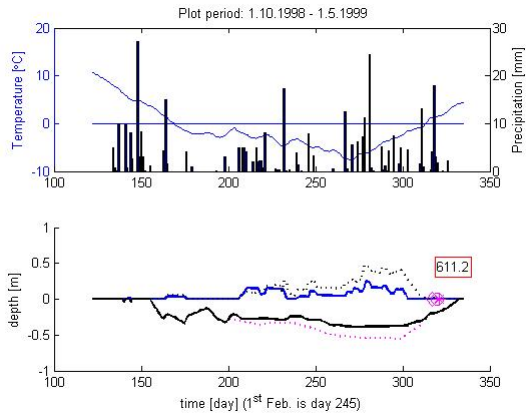


Figure 9f. Simulation results for the winter of 1998-1999.

temperature throughout the year, evaluation of model performance, and model testing at different locations in Norway covering different climatic conditions. The main purpose of **SnowFrost** is to simulate winter conditions within a plant model in order to study the winter survival of forage crops. Thus **SnowFrost** must meet the requirements of the plant model.

We conclude that the results shown in figures 9a-9f are quite promising, and that **SnowFrost** is suitable as a foundation for the continuing work. In order to get an impression of how new versions of the model perform, we will compare our simulation results with results from the Swedish COUP-model of Jansson and Karlberg (2001) using the same parameterisation.

# Appendix A Symbols

# Appendix B Energy Transport in the Soil

The soil temperature in is governed by energy supply from the surroundings, and the thermal conductivity of the soil. The thermal conductivity $\lambda_g$ is the main mechanism for energy transfer in the soil, and thus knowledge about this parameter is of great importance. This $\lambda_g$ can either be estimated from temperature and soil water content measurements at different depths in the soil profile, or calculated from empirical expressions (Hillel, 1980).

## B.1 Fourier's Law

Fourier's law describes the conduction of heat in a medium. This law says how the temperature varies with time and distance in a heated medium, for instance a heated rod.

### B.1.1 Example

As a one-dimensional example, we can envisage a rod of a homogenous material. Assume that the cross section area *A* is perpendicular to the length of the rod, and that temperature *T* is constant on each cross section. Assume also that the rod's lateral surface is insulated, and no heat can pass through this surface. Then heat will flow through the rod in a fluid-like manner from warmer to cooler sections. The **heat flux density** *Q* at position z and time *t* in this rod is the *rate of flow of heat across a unit area* of a cross section of the rod at position z. The result is the empirical principle known as Fourier's law (Edwards & Penney, 2004), which in one-dimensional form is

**Equation 15**

$$Q = -\lambda \frac{\partial T}{\partial z}$$

where *Q* is the heat flux density in the direction of z, the temperature function *T(z,t)* describes the rod's temperature in position z at time *t*, and the proportionality constant $\lambda$ is the thermal conductivity of the rod. The negative sign indicates that energy flows from higher to lower temperatures. Fourier's law takes the general form

**Equation 16**

$$Q = -\lambda \nabla T$$

where $\nabla T$ is the temperature gradient in the medium, and $\lambda$ is the thermal conductivity of the medium. Equation (16) can be used to describe e.g. the spatial variation of temperature in soil.

## B.2 Derivation of the Heat Equation

Suppose we have a rod like the one described in the example above. We have a cross section area *A* [$m^2$] of the rod, the density of the rod $\rho$ [kg $m^{-3}$], the specific heat of the rod *c* [J $kg^{-1}$ $K^{-1}$] (the amount of energy required to raise 1 kg of the rod 1 °C), and the temperature in position z at time *t*, described by the continuous function *T(z,t)*. We now take a look at a small increment along the length of the rod Δz, i.e. the interval [z, z + Δz]. The rate *F* at which energy accumulates in this segment of the rod can be expressed as follows

**Equation 17**

*F = {energy in} - {energy out}*

$$= AQ(z,t) - AQ(z+\Delta z,t)$$
$$= \lambda A\left[T_z(z+\Delta z,t) - T_z(z,t)\right]$$

where $T_z$ denotes $\frac{\partial T(z,t)}{\partial z}$. The time rate of change of the temperature, that is $T_t$, is related to both density $\rho$ and specific heat *c*, so we need an expression that incorporates these two. From the expression of specific heat *c*, we know that the amount of energy required to raise the temperature of 1 $m^3$ of the rod from 0°C to temperature *T* is given by the product $(c\rho T)$. The length of a tiny slice of the rod segment is dz, and the volume of this slice is $(Adz)$, and thus the required amount of energy to heat this slice from 0°C to temperature *T* is given by the product

$\left( c\rho TAdz \right)$. Now, to find the **heat content** *Φ* of the rod segment, we integrate over all the slices that comprise the segment's length Δz

**Equation 18**

$$\Phi(t) = \int_{z}^{z+\Delta z} c\rho AT(z,t)\mathrm{d}z$$

The rod being insulated on the lateral surface, illustrates the *principle of energy conservation*[1], and the *equation of continuity* [2].
Equation (17) expresses the rate at which energy enters and leaves the rod segment. Since *Φ* is the heat content, and *F* (from equation (16)) is the rate of heat flow, we can obtain an expression for the rate of change in heat content as follows

**Equation 19**

$$\frac{\mathrm{d}\Phi}{\mathrm{d}t} = \lambda A\left[T_z(z+\Delta z,t) - T_z(z,t)\right]$$

A second way to express this change in heat content is to differentiate the temperature function *T(z,t)* with respect to *t* in equation (18) *within* the integral, and then applying the *Mean Value Theorem for Definite Integrals* (see Appendix C) to solve the integral

**Equation 20**

$$\frac{\mathrm{d}\Phi}{\mathrm{d}t} = \int_{z}^{z+\Delta z} c\rho AT_t(z,t)\mathrm{d}z$$
$$= c\rho AT_t(\bar{z},t)\Delta z$$

where $\bar{z}$, from the interval *(z, z + Δ)*, is the z value that produces

$$\int_{z}^{z+\Delta z} T_t(z,t)\mathrm{d}z = T_t(\bar{z},t)\Delta z$$

Now we can equate equations (19) and (20)

**Equation 21**

$$c\rho AT_t(\bar{z},t)\Delta z = \lambda A\left[T_z(z+\Delta z,t) - T_z(z,t)\right]$$
$$\Downarrow$$
$$T_t(\bar{z},t) = \frac{\lambda}{c\rho}\frac{\left[T_z(z+\Delta z,t) - T_z(z,t)\right]}{\Delta z}$$

By taking the limits as $\bar{z} \to z$ and $\Delta z \to 0$, and introducing the *thermal diffusivity* constant $D_T$

$$D_T = \frac{\lambda}{c\rho}$$

we obtain the resulting one-dimensional *heat equation*

**Equation 22**

$$\frac{\partial T}{\partial t} = D_T \frac{\partial^2 T}{\partial z^2}$$

We can use equation (22) to calculate heat transport in the soil. The three parameters *thermal conductivity* $\lambda_s$ , *heat capacity* c and *thermal diffusivity* $D_T$ are often referred to as the thermal properties of the soil (Hillel, 1980).

[1] Energy can neither be created nor destroyed.
[2] This equation says that energy entering the medium at one rate must exit the medium at the same rate, assuming there are no places between entry and exit points to add or remove energy.

# Appendix C **Mean Value Definite Integral**

We can define the average value of a continuous function *f(x)* over a closed interval [*a, b*] as the *definite* integral $\int_a^b f(x)dx$ divided by the length of this interval. The Mean Value Theorem for Definite Integrals says this average value *always* occur at least once in the interval.

**Theorem 1.**
*If the function f is continuous on the closed interval* [*a, b*]*, then at some point* $c \in [a,b]$

$$f(c) = \frac{1}{b-a}\int_a^b f(x)dx$$

## References

Colleuille, H., Gillebo, E. 2002. Nasjonalt observasjonsnett for markvann. NVE Rapport nr.6, 64 pp.

Edwards, C.H., Penney, D.E. 2004. Differential Equations and Boundary Value Problems. Pearson Prentice Hall, USA

Førland, E.J. (ed), Allerup, P., Dahlström, B., Elomaa, E., Jónsson, T., Madsen, H., Perälä, J., Rissanen, P., Vedin, H., Vejen, F. 1996. Manual for operational correction of Nordic precipitation data. Report 24, Norwegian Meteorological Institute, 66 pp.

Grønås, S. 2005. Norges klima om hundre år – usikkerheter og risiko. Cicerone 2005(4): 20-21.

Hillel, D. 1980. Introduction to Soil Physics. Academic Press, Inc. USA

Jansson, P.E., Karlberg, L. 2001. Coupled heat and mass transfer model for soil-plant-atmosphere systems. Royal Institute of Technology, Dept of Civil and Environmental Engineering, Stockholm, Sweden, 321 pp.

Johansen, Ø. 1976. Grunnlag for termisk dimensjonering. In: Sætersdal, R. (ed.) Frost Action in Soils no 17, pp.25-34. Norges Teknisk-Naturvitenskapelige Forskningsråd og Statens Vegvesens utvalg for frost i jord, Oslo, Norway.

Kennedy, I., Sharrat, B. 1998. Model Comparisons to Simulate Soil Frost Depth. Soil Science. Vol 163 (8), pp. 636-645

McCarthy, J.J, Canziani, O.F., Leary, N.A., Dokken, D.J., White, K.S. (editors). 2001. Climate change 2001: Impacts, Adaption, and Vulnerability. Cambridge University Press. 1032 pp.

Melloh, R.A. 1999. A Synopsis and Comparison of Selected Snowmelt Algorithms. US Army Corps of Engineers. Cold Regions Research & Engineering Laboratory. CRREL Report 99-8.

Olsen, P.A., Haugen, L.E. 1997. Jordas Termiske Egenskaper. Report no.8/97 (58), Norwegian Agricultural University, JVP, ISSN 0805-7214.

Riley, H., Bonesmo, H. 2005. Modelling of snow and freeze-thaw cycles in the EU-rotate N decision support system. Planteforsk grønn kunnskap (9) 112

Van Oijen, M., Höglind, M., Hanslin, H.M., Caldwell, N. 2005. Process-Based Modelling of Timothy Regrowth. Agronomy Journal 97 (5): 1295-1303

| Symbol | Quantity | SI Units | Parameter Value |
|---|---|---|---|
| $A$ | Unit area | $m^2$ | 1 |
| $C_{cum}$ | Empirical parameter used for $f_{cap}$ calculation | $m^3\ kg^{-1}$ | 0.36 |
| $f_{cap}$ | Retention capacity of snow cover | | |
| $f_{capMax}$ | Maximum retention capacity of snow cover | | 0.17 |
| $f_{capMin}$ | Minimum retention capacity of snow cover | | 0.04 |
| $f_w$ | Fraction of liquid water in precipitation | | |
| $\gamma$ | Empirical parameter | | 65 |
| $F_{depth}$ | Simulated lower boundary of soil frost | m | |
| $K_{cum}$ | Empirical parameter used for $K_m$ calculation | $m\ mm^{-1}$, $m^3\ kg^{-1}$ | 0.99 |
| $K_f$ | Degree-day-factor for refreezing | $mm\ °C^{-1}\ day^{-1}$ | 1.5 |
| $K_M$ | Degree-day-factor for snowmelt | $mm\ °C^{-1}\ day^{-1}$ | |
| $K_{max}$ | Maximum value for $K_M$ | $mm\ °C^{-1}\ day^{-1}$ | 6.19 |
| $K_{min}$ | Minimum value for $K_M$ | $mm\ °C^{-1}\ day^{-1}$ | 4.0 |
| $L_f$ | Latent heat of fusion | $kJ\ kg^{-1}$ | 335 |
| $\lambda_g$ | Thermal conductivity of soil (both *unfrozen* and frozen) | $W\ m^{-1}\ K^{-1}$ | 2.0 |
| $\lambda_s$ | Thermal conductivity of snow cover | $W\ m^{-1}\ K^{-1}$ | 0.2 |
| $M$ | Rate of snowmelt | $mm\ day^{-1}$ | |
| $M_f$ | Rate of snowmelt that refreezes within snow cover | $mm\ day^{-1}$ | |
| $m_w$ | Mass of water in a soil volume | kg | |
| $P$ | Measured precipitation rate | $mm\ day^{-1}$ | |
| $P_r$ | Precipitation as rain | $mm\ day^{-1}$ | |
| $P_s$ | Precipitation as snow | $mm\ day^{-1}$ | |
| $perDay$ | Empirical parameter | $day^{-1}$ | |
| $Q_E$ | Latent heat flux density | $W\ m^{-2}$ | |
| $Q_{fs}$ | Heat flux density through frozen soil layer | $W\ m^{-2}$ | |
| $Q_g$ | Geothermal heat flux density | $W\ m^{-2}$ | 3.47 |
| $\rho_{pack}$ | Empirical parameter for snow densification | $m\ m^{-1}\ day^{-1}$ | 0.02 |
| $\rho_{snow}$ | Density of snow cover | $kg\ m^{-3}$ | |
| $\rho_{snowNew}$ | Density of fresh snow | $kg\ m^{-3}$ | 100 |
| $\rho_w$ | Density of water | $kg\ m^{-3}$ | 1000 |
| $S_{depth}$ | Simulated depth of snow cover | m | |
| $S_{dry}$ | Amount of water in solid phase in snow cover | mm | |
| $S_{wet}$ | Amount of water in liquid phase in snow cover | mm | |
| $SWE$ | Snow water equivalent | mm | |
| $t$ | Simulation time step | day | |
| $T_{air}$ | Daily average air temperature | °C | |
| $T_{surf}$ | Air temp. between soil surface and snow over | °C | |
| $T^*$ | Freezing temperature of soil water | °C | 0 |
| $T(z,t)$ | Soil temperature at depth z at time $t$ | °C | |
| $T_{upper}$ | Upper critical air temperature | °C | 1.0 |
| $T_{low}$ | Lower critical air temperature | °C | -3.0 |
| $T_{bm}$ | Lower base temperature for snow melt | °C | 0.7 |
| $T_{bf}$ | Lower base temperature for refreezing | °C | -1.4 |
| $V$ | Unit volume of soil | $m^3$ | 1 |

| Symbol | Quantity | SI Units | Parameter Value |
|---|---|---|---|
| $W_{out}$ | Rate of liquid water on soil surface | mm $day^{-1}$ | |
| $x_w$ | Volume fraction of liquid water in soil | | 0.4 |
| $z$ | Soil depth | m | |
| $\zeta$ | Thickness of frozen soil layer | m | |

**Tabel 2: Table of symbols used in the report on the SnowFrost model.**